

A Study on Power Distribution Improvement using the Form Function in a Molten Salt Fast Reactor with a Local Moderator

Sungtaek Hong^a, Junwoo Lee^b and Yonghee Kim^{b*},

^aKorea Atomic Energy Research Institute, 111, Daedeok-daero 989beon-gil, Yuseong-gu, Daejeon, Republic of Korea

^bKorea Advanced Institute of Science and Technology, 291 Daehak-ro, Yuseong-gu, Daejeon, Republic of Korea

*Corresponding author: yongheekim@kaist.ac.kr

***Keywords :** Molten Salt Fast Reactor(MSFR), Moderator, Power distribution, Form function

1. Introduction

One of the core reactor concepts of the Generation IV International Forum (GIF), the Molten Salt Reactor (MSR) [1], offers outstanding advantages such as low-pressure operation, the use of liquid fuel, high inherent safety, and superior fuel utilization efficiency. In particular, to overcome the burnup limitations of conventional thermal-spectrum MSRs, active research on the Molten Salt Fast Reactor (MSFR) [2] is being conducted worldwide.

Previous studies [3][4] have shown that, in MSFR reactivity calculations, significant discrepancies of several hundred pcm arise between the Neutron Diffusion Equation (NDE) and Monte Carlo methods. This indicates that conventional diffusion theory alone has inherent limitations in accurately describing the complex neutron behavior characteristic of MSFR systems. As a practical alternative, a multi-group diffusion approach based on the Simplified Generalized Equivalence Theory (Simplified GET) [5] has been proposed.

However, for MSFR models in which the reflector region contains moderator material [6], steep neutron flux gradients at the core-reflector interface make it difficult to avoid errors in the predicted power distribution near the reflector boundary.

In this study, a form function is introduced to accurately capture of the power distribution. By coupling microscopic power distribution characteristics with macroscopic diffusion calculation results, the form function plays a crucial role in substantially enhancing computational accuracy.

2. Methods and Results

2.1 Reactor Model

The reactor model used in this study is shown in Figure 1. In the figure, gray represents the fuel, green represents the moderator, yellow indicates the side reflector, and orange denotes the top and bottom reflectors.

The reactor fuel consists of a 46KCl-54UCl₃ composition. Structurally, the top and bottom are surrounded by stainless steel reflectors. On the lateral

side, the moderator surrounds the nuclear fuel, and an additional reflector encloses the outer region of the moderator.

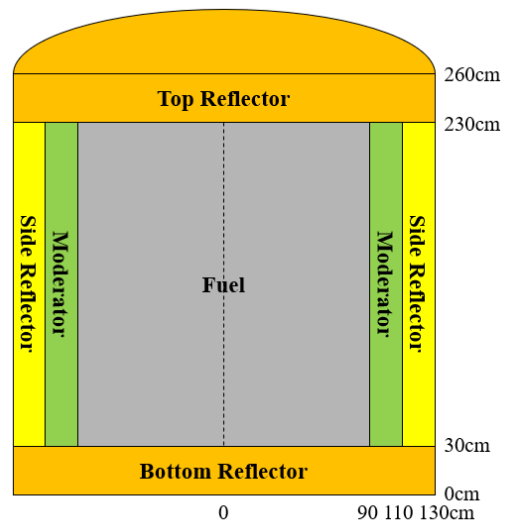


Fig 1. MSFR with a Local Moderator

2.2 Reactor Materials

The materials utilized in this reactor are consistent with those from a previous investigation [2], except for the U-235 fuel concentration which is now 19.75 wt.%. Additionally, BeO has been added as a moderating reflector. The materials information is provided in Table I.

Table I. Materials Data

| Materials | Data |
|-------------------------|--------------------------|
| Fuel salt | 46KCl-54UCl ₃ |
| Fuel salt melting point | 831 K |
| Fuel density | 3.78912 g/cc |
| Fuel temperature | 923 K |
| Enrichment of U-235 | 19.75 wt.% |
| Enrichment of Cl-37 | 99.0 at.% |
| Reflector | Stainless steel 304 |
| Reflector density | 8.0 g/cc |
| Reflector temperature | 823 K |

| | |
|-----------------------|-----------|
| Moderator | BeO |
| Moderator density | 3.01 g/cc |
| Moderator temperature | 823 K |

2.3 Power Reconstruction of Reactor

The fundamental principle of power reconstruction using a form function is to superimpose a form function - representing the local heterogeneous characteristics of a given region - onto the nodal homogenized neutron flux or power distribution obtained from core calculations. In this way, fine-scale spatial variations that cannot be captured by homogenized nodal solutions alone can be effectively recovered. A schematic representation of the reconstruction methodology is depicted in Figure 2.

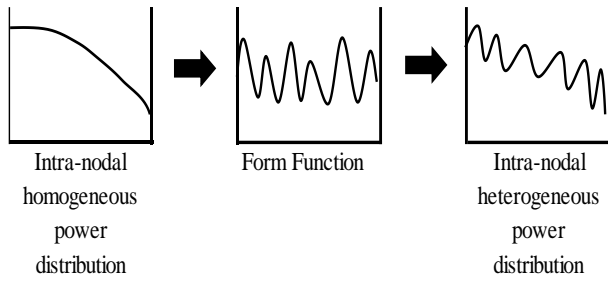


Figure 2. Conceptual schematic of intra-nodal power reconstruction using form functions

It should be noted that this technique is applied as a post-processing step after the core neutronic calculation has been completed. Consequently, the application of the form function does not alter the previously calculated effective multiplication factor (k_{eff}).

By combining the homogenized core solution with a properly defined form function, numerical errors observed in the core can be efficiently mitigated without incurring the substantial computational cost associated with a fully heterogeneous core calculation.

To reconstruct the local power distribution within a given region, the form function is defined by normalizing the fine-mesh power values. Let p_i denote the local power at fine-mesh cell i within a given spectral geometry. Then, the form function F_i for the i -th fine node is expressed as the ratio of the local fine-mesh power to the average power over the region, ensuring that the integral of the form function over the node is preserved.

This mathematical definition is given in Eq. (1):

$$F_i = \frac{p_i}{\sum_{j=1}^N p_j}, \quad (1)$$

where,

N: the total number of fine-mesh nodes within the target region of the spectral geometry.

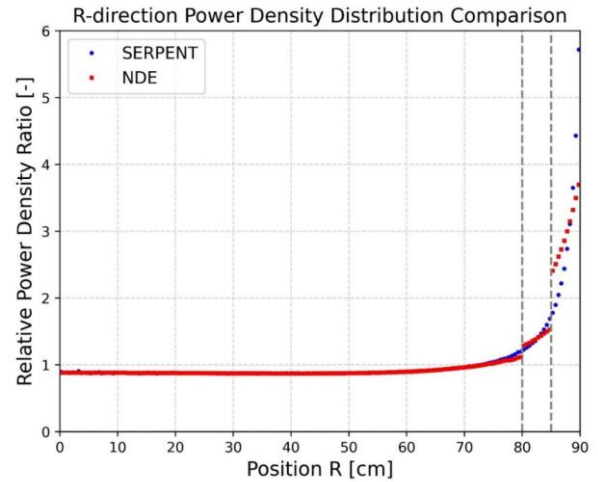


Figure 3. Power distribution comparison

In this study, the form function was applied to the radial fuel region between 85 and 90 cm, where numerical errors in the power distribution exceeded 10%. As shown in Figure 3, the errors in the 85 - 90 cm region exhibit a positive bias to the left of the mean and a negative bias to the right. The blue dots represent the reference solution obtained using SERPENT, while the red dots denote the solution calculated by implementing the Simplified GET method.

When deriving the form function, an infinite cylinder model and a corner region model were employed according to the characteristics of the target region. A key advantage of the present methodology is that it does not require any additional Monte Carlo calculations for generating the form function. Instead, the results already obtained from the characterization of spectral geometry - a fundamental step within the Simplified GET calculation process - were directly utilized, thereby maximizing computational efficiency.

Table II. Infinite cylindrical spectral geometry-based form functions for the initial core

| Radial Position | F_i |
|-----------------|--------|
| 85.25 | 0.0586 |
| 85.75 | 0.0608 |
| 86.25 | 0.0663 |
| 86.75 | 0.0741 |
| 87.25 | 0.0798 |
| 87.75 | 0.0908 |
| 88.25 | 0.1043 |
| 88.75 | 0.1201 |
| 89.25 | 0.1516 |
| 89.75 | 0.1936 |

Using the infinite cylinder model, power values were extracted and normalized in 0.5 cm increments for the radial region between 85 and 90 cm; these normalized values were then multiplied by the power values obtained via the Simplified GET method to reconstruct

the power distribution of the corresponding area. However, for the regions where the top and side reflectors meet, a corner model was separately developed. The form functions for these areas were specifically derived from the corner model and then applied.

Table II presents the form functions derived from the infinite cylinder spectral geometry. The form functions were generated at 0.5 cm intervals along the radial direction. The radial positions are represented by the midpoint values of each respective interval; for instance, the value 85.25 cm denotes the spatial region ranging from 85.0 to 85.5 cm.

Table III. Corner spectral geometry-based form functions for the initial core

| Axial Radial | 228.75 | 226.25 | 223.75 | 221.25 | 218.75 | 216.25 |
|-----------------|--------|--------|--------|--------|--------|--------|
| 85.25 | 0.010 | 0.010 | 0.011 | 0.011 | 0.012 | 0.012 |
| 85.75 | 0.011 | 0.011 | 0.011 | 0.012 | 0.012 | 0.013 |
| 86.25 | 0.011 | 0.012 | 0.012 | 0.013 | 0.013 | 0.014 |
| 86.75 | 0.012 | 0.012 | 0.013 | 0.014 | 0.014 | 0.015 |
| 87.25 | 0.012 | 0.013 | 0.014 | 0.015 | 0.016 | 0.016 |
| 87.75 | 0.013 | 0.014 | 0.015 | 0.016 | 0.017 | 0.018 |
| 88.25 | 0.014 | 0.016 | 0.017 | 0.018 | 0.019 | 0.020 |
| 88.75 | 0.016 | 0.018 | 0.019 | 0.021 | 0.022 | 0.023 |
| 89.25 | 0.018 | 0.020 | 0.023 | 0.024 | 0.026 | 0.027 |
| 89.75 | 0.022 | 0.025 | 0.028 | 0.030 | 0.033 | 0.034 |

Similarly, Table III lists the form functions derived from the corner model spectral geometry. Since the corner model was developed using a two-dimensional configuration, the resulting form functions are likewise expressed as two-dimensional functions. In the case of the corner model, the form functions were generated at 0.5 cm intervals in the radial direction and 2.5 cm intervals in the axial direction. For instance, the axial value of 228.75 cm represents the region extending from 227.5 to 230.0 cm. Due to the axial symmetry of the reactor model with respect to its center, the same form functions were applied to the lower corner region (30 - 45 cm).

2.4 Results

Based on Figure 1, the form functions were applied to the radial region between 85 and 90 cm. Specifically, the corner spectral geometry-based form functions summarized in Table III were applied to the axial (Z-direction) regions of 30–45 cm and 215–230 cm, while the Infinite cylindrical spectral geometry-based form functions presented in Table II were utilized for the remaining areas. For the depleted (burned) core case,

form functions based on both infinite cylindrical and corner spectral geometries were similarly derived and applied.

Table IV presents the power distribution and peak power errors before and after applying the form functions. The power distribution errors, which were previously high at the fuel periphery, were reduced to approximately 10% after applying the form functions. Furthermore, the peak power error was significantly improved, dropping from around 40% to less than 5%.

Table IV. Power distribution and peak power results with and without form functions

| | Power distribution | | Peak power | |
|--------------|--------------------|------------------|------------|--------|
| | Before | After | Before | After |
| Initial Core | -35.2 % ~ 42.9% | -6.9% ~ 10.5% | -35.2% | -1.12% |
| Burned core | -46.8% ~ 65.9% | -6.7% ~ 13.1% | -46.8% | -1.26% |

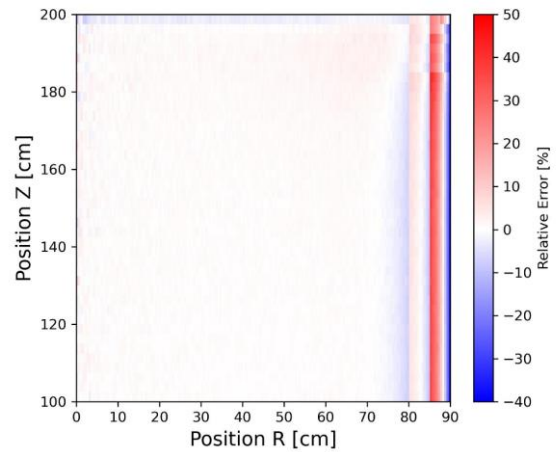


Fig 4. Power distribution errors in the initial core prior to the incorporation of form functions

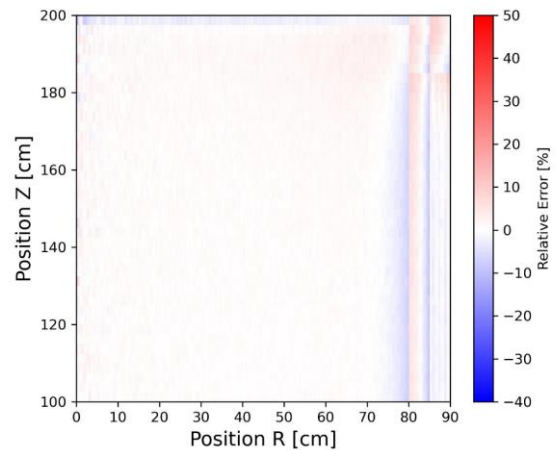


Fig 5. Power distribution errors in the initial core after the incorporation of form functions

Figures 4 and 5 illustrate the improvement effects for the initial core, while Figures 6 and 7 show those for the depleted (burned) core. Similar to Figure 3, Figures 4 and 6 exhibit a positive bias near 85 cm and a negative bias near 90 cm. However, Figures 5 and 7, which present the results after applying the form functions, show that these errors in the corresponding regions have been significantly reduced.

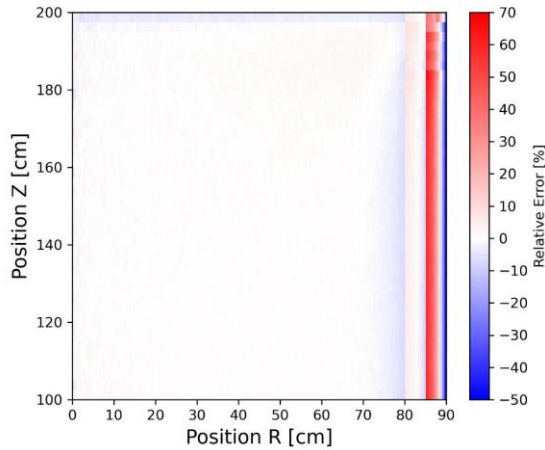


Fig 6. Power distribution errors in the burned core prior to the incorporation of form functions

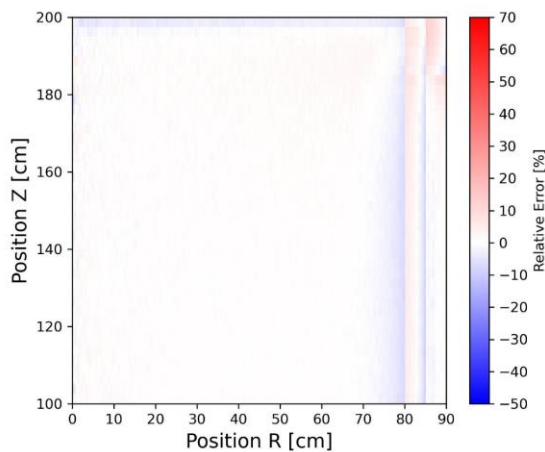


Fig 7. Power distribution errors in the burned core after the incorporation of form functions

3. Conclusions

In this study, a power reconstruction methodology using form functions was developed and evaluated to enhance the accuracy of power distribution predictions in a MSFR. The investigation confirmed that significant numerical discrepancies, exceeding several tens of percent, occurred primarily at the fuel-reflector interface in the radial region between 85 and 90 cm. To

mitigate these errors, form functions were derived using infinite cylinder and corner region spectral geometry models, which were then coupled with diffusion results obtained via the Simplified GET.

The application of this methodology yielded a substantial improvement in computational fidelity. After implementing the form functions, the power distribution errors at the fuel periphery were reduced to approximately 10%. Also, the peak power error, which was initially as high as 40%, was significantly improved to less than 5%. A major advantage of this approach lies in its computational efficiency; by directly utilizing the pre-existing spectral geometry-based results, the need for additional, time-consuming Monte Carlo simulations for form function generation was eliminated. Furthermore, the consistent performance of the proposed method across both initial and burned core states demonstrates its robustness and versatility for various reactor operating conditions.

Acknowledgments

This research was supported by the National Research Foundation of Korea (NRF) grant funded by the Korean Government (MSIP) (2021M2D2A207638322), and by a Korea Energy Technology Evaluation and Planning (KETEP) grant funded by the Korean government (MCEE) (RS-2024-00439210).

REFERENCES

- [1] "Molten salt reactor", <https://www.gen-4.org/>
- [2] Sungtaek Hong, Seongdong Jang, Taesuk Oh & Yonghee Kim, "Preliminary Study on the Candidate Fuel Salt of Molten Chloride Salt Fast Reactor", Korean Nuclear Society Virtual Spring Meeting (2021)
- [3] Eric Cervi et al., "Multiphysics analysis of the MSFR helium bubbling system: A comparison between neutron diffusion, SP3 neutron transport and Monte Carlo approaches", *Annals of Nuclear Energy*, 132, 227-235 (2019)
- [4] Sungtaek Hong, Seongdong Jang, Taesuk Oh & Yonghee Kim, "A Study on the Application of Equivalence Theory to Molten Salt Fast Reactor", Korean Nuclear Society Autumn Meeting (2022)
- [5] Sungtaek Hong et al., "A study on the applicability of simplified few-group GET (Generalized Equivalence Theory) to cylindrical molten salt fast reactor", *Nuclear Engineering and Technology*, 56(10), 4207-4218 (2024).
- [6] Sungtaek Hong & Yonghee Kim, "A Study on the Applicability of Simplified GET Theory to MSFR with Local Moderator", Korean Nuclear Society Spring Meeting (2023)